Transactions of the Materials Research Society of Japan Vol.28 101-106 (2003)

XAFS Study of Thin Films Fabricated with Cluster Ion Assisted Deposition Technique

Jiro Matsuo[1)], Teruyuki Kitagawa[2,5)], Yutaka Shimizugawa[2,3)], Hiroyuki Kageyama[4)], Kazuhiro Kanda[2)], Toshio Seki[1,5)], Takaaki Aoki[1,5)], Shinji Matsui[2)] and Isao Yamada[2,5)]

[1)] Quantum Science and Engineering Center, Kyoto University, Kyoto 606-8501, JAPAN

Fax: 81-75-753-3571, e-mail: matsuo@nucleng.kyoto-u.ac.jp

[2)] Laboratory of Advanced Science and Technology for Industry, Himeji Institute of Technology

[3)] New Energy and Industrial Technology Development Organization (NEDO)

[4)] National Institute of Advanced Industrial Science and Technology

[5)] Collaborative Research Center for Cluster Ion Beam Process

A novel method employing Gas Cluster Ion Beam (GCIB) assisted deposition was developed to deposit hard carbon films. C_{60} was used as a carbon source and Ar cluster ion beam bombarded onto C_{60} to form hard carbon film. The carbon films deposited at 7keV GCIB showed much higher hardness than films deposited with other technique. Electron energy loss spectra (EELS), near edge X-ray adsorption fine structure (NEXAFS) and Raman spectroscopy were used to investigate the chemical bonding configuration of the films. Local structure around Sn ion in indium tin oxide (ITO) thin films deposited with O_2 cluster ion assisted technique were investigated by Sn K XAFS. Sn K XAFS spectra were measured in both transmission and a fluorescent technique Sn Kα fluorescence signal from 19 elements solid-state detector could be picked up from In Kα fluorescence, In Kβ fluorescence, Sn Kβ fluorescence and elastic scattering signals. Local structure around Sn atoms in ITO is completely different from tin oxide structure. The first neighbor Sn-O distance was slightly increased with substrate temperature during deposition. The oxygen coordination number of Sn and the second neighbor Sn-In (Sn) peak area also increased with substrate temperature.

Key words: cluster, ion, XAFS, Raman, EELS

1. INTRODUCTION

Clusters, aggregates of atoms or molecules, are of interest not only as a new state of matter but also as a new material process, which has been developed at Kyoto University [1-20]. When a cluster with the size of 1000 atoms is accelerated with energy of 10 keV, each constituent atom has only 10 eV, and these 1000 atoms collide with the surface within a several nm^2. Thus, cluster ions with a low equivalent energy (low velocity) impact on solid surfaces with extremely high energy and particle density.

Because of these high-density energy deposition and multiple-collisions on surfaces, the collision of the energetic cluster on an atomistic scale is still unclear. Traces of single ion impact on surfaces have been observed with Scanning Tunneling Microscope (STM) for both monomer ions and cluster ions.[15,16] One clear evidence of cluster effects (peculiarity of clusters) is the crater formation on solid surfaces.

The cluster effects can to be utilized for various material processes, such as surface smoothing, high-quality thin film formation, high rate sputtering, nano-etching and very shallow implantation [9,10]. Especially, surface smoothing is one of the promising technologies for industrial applications. Surface smoothing effect with cluster ion beam has been reported for various materials, such as , semiconductors and diamond[11,14] Scratches on surfaces can be also removed. It has been demonstrated that surface smoothing process is able to improve characteristics of magnetic tunnel junction (MTJ), which will be utilized for next generation tunneling magnetoresistance (TMR) read head.[18]

Another important application is thin film formation. The ion assisted deposition technique is widely used for industrial applications. Due to the damage formation with high-energy ions, the energy of the assisted ions has to be as low as possible. Formation of Diamond Like Carbon (DLC) film and tin–doped indium-oxide (ITO) film using GCIB have been demonstrated [4-8].

Hard carbon films (e.g. DLC: diamond-like carbon) have been used in the last decade for a number of applications, because of their superior properties, which include not only high hardness but also low friction coefficient, transparency and chemical stability [21,22].

However DLC films deposited by present technologies have a limited range of applications. In view of the remarkable recent progress in the field of electronics and hard coatings, good properties are required for various devices in the next generation [23], and thus improvements in DLC deposition technique are also required.

We have proposed a novel method employing gas cluster ions beam (GCIB) assisted deposition as a breakthrough in DLC synthesis. In this method, energetic gas cluster ions deliver extremely high energy

densities into very localized and shallow atomic level regions of a substrate surface [16]. Because the impact point of a cluster ion for an instant attains conditions of high pressure and high temperature [17], Molecular Dynamic simulation reveals that the phase transition from sp^2 to sp^3 is enhanced even when the substrate is held at room temperature. As well, it is expected that films with quite smooth surfaces can be achieved with the lateral sputtering effect that is a unique characteristic of cluster ion bombardment [3,13]. One of the difficulties in development in DLC film deposition is that very few analysis techniques are available to study the chemical bonding state of the carbon atom.

Tin doped indium oxide (ITO) films are known to be transparent conductive films that have high electrically conductivity and are highly transparent in the visible region. Therefore they are widely applied to optoelectronic devices such as flat displays or solar cells. For this purpose, a new gas cluster ion deposition technique has been developed. Using indium and tin metal as deposition sources, high quality ITO films were deposited with oxygen gas cluster ion assistance.

The carrier in ITO film is created when Sn^{4+} ion is substituted In^{3+} ion. Therefore, the resistivity of ITO film is concerned with coordination state of Sn ions. To develop the high-quality ITO films, coordination states of Sn ions have to be investigated. X-ray absorption fine structures (XAFS) analysis is a powerful method to investigate the local structure around the particular ion in multi-component materials. In this study, Sn K XAFS measurements of ITO films, which were obtained by O_2 gas cluster ion assisted deposition technique, as a function of substrate temperature.

2. EXPERIMENTS

A schematic diagram of the apparatus for cluster ion assisted deposition is shown in figure 1. Carbon films were formed by evaporating C_{60} as a carbon source from heating crucible and Ar cluster ion bombard C_{60} on the surface simultaneously. In case of ITO film deposition, ITO pellets were used for evaporation and O_2 cluster ions were bombarded to form high-quality oxide films. The Ar and O_2 clusters were formed by adiabatic expansion of high-pressure gas through a small nozzle into high vacuum.[8,24,25] The neutral clusters were

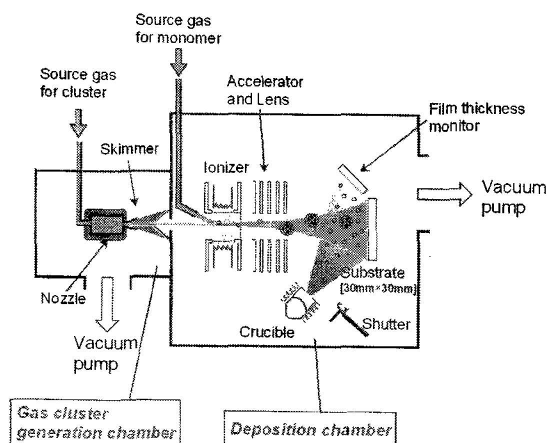

Figure 1 Schematic Diagram of Cluster Ion Assisted Deposition System

introduced to an ionizer through a skimmer, and ionized by electron bombardment. Subsequently cluster ions were accelerated up to 9 keV. The mean size of the cluster ion was 1000 atoms/ion. Therefore in the case of an acceleration energy of 9 keV, the energy per atom was 9eV. The evaporation rate was measured with a quartz thickness monitor.

Hardness of the DLC films was measured by the nano-indentation technique (Hysitron Inc.: Tribo-Scope). The hardness of each film was obtained as an average of 5 measurements. Bonding structures of the films were studied with EELS, NEXAFS and Raman spectroscopy. The wavelength of the excitation laser for Raman spectroscopy was 532 nm. The amount of sp^2 ratio in the carbon film was evaluated with electron energy loss spectroscopy (EELS) with electron energy of 200 kV. The NEXAFS measurement was useful to obtain information of the sp^2-hybridized orbital content in DLC films [20,26]. NEXAFS measurements were performed using synchrotron radiation. Soft X-ray generated from synchrotron radiation was irradiated to the film at normal incidence with photon energy from 275 to 320 eV. Total electron yields were counted]for all electrons emitted from the surface. The sp^2 content in carbon films was analyzed by using the near edge peak of p* resonance (285.5 eV), with a reference from the spectrum of graphite.

In and Sn K XAFS spectra were measured in transmission and florescence mode using a Si (111) double crystal monochromator at BL01B1 at SPring-8. The sample for transmission measurement near In and Sn K edge was 50μm thickness of ITO film deposited by electron beam on 20μm of silica glass. Harmonics were rejected by a grazing incidence mirror. A mixture of argon (75 %) and krypton (25 %) was filled in the I_0 ionization chamber, and a mixture of argon (50 %) and krypton (50 %) in the I ionization chamber. The scan time for one data-point was one second. Absorption spectra of metallic In and Sn, SnO, SnO_2 and bixbyite-type In_2O_3 were also measured.

Sn K XAFS spectra of ITO films with low resistivity were measured in a fluorescent mode. In order to increase sensitivity, a 19 elements solid state detector (SSD) was used for I detection. Single channel analyzers were utilized to pick up Sn Kα fluorescence signal from In Kα fluorescence, In Kβ fluorescence, Sn Kβ fluorescence and elastic scattering signals. The scan time for one data-point was 20 seconds. The sum of all available elements data was used for analysis. A counting loss of SSD was accounted for in the analisys.

3. RESULTS AND DISCUSSION

3.1 DLC films

EELS and NEXAFS were used to anaylize various DLC films. DLC films were deposited by Ion Plating, ECR(Electron Cyclotron Resonance) and Cluster Ion Assisted technique. Graphite was also measured as a reference sample of pure sp^2 bonded material. In principle, both EELS and NEXAFS spectra should be similar, because the same electronic transitions are measured with both techniques.

Figure 2 shows the EELS and NEXAFS spectra of various DLC films. DLC films have two different

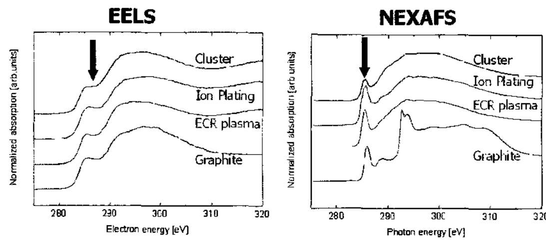

Figure 2 Comparison of EELS and NEXAFS of various DLC samples. The energy resolution of NEXFAFS is much better than that of EELS. The arrow near the peak at 285.5eV is assigned to excitation from 1S to sp^2 bond

bonding states of sp^2-hybridized bond and sp^3-hybridized bond. The peak at 285.5eV is assigned to excitation from 1S to sp^2 bond [27]. When this peak (285.5eV) is high, it indicates a large fraction of sp^2 bond in films. Because diamond have only sp^3 bond, there is no peak at this energy. Therefore, lower height of this peak indicates diamond-like properties in films. In order to analyze the amount of sp^2 bond in the film, the integrated intensity of the peak at 285.5eV was normalized by the background intensity.

As shown in figure 2, NEXAFS spectra have a much better energy resolution than EELS spectra. Many peaks are found in the NEXAFS spectrum of graphite. In contrast with NEXAFS spectra, only one peak at 286eV is found in EELS spectra. In the cluster ion assisted deposition technique, degradation of sp^2 peak is clearly observed in NEXAFS spectra. However,a slight difference in the same peak was found in EELS spectra. Therefore, NEXAFS is much more suitable to study the chemical bonding configuration in DLC films.

Figure 3 shows NEXAFS spectra of DLC films formed by various deposition techniques. A C_{60} film is also presented in figure 3. The NEXAFS spectrum of the C_{60} film shows three p* peak near the carbon K edge (284.5eV, 285.5 eV, and 287.4 eV). This result agrees well with the previous theoretical study [28]. The spectrum of the film formed with C_{60} evaporation

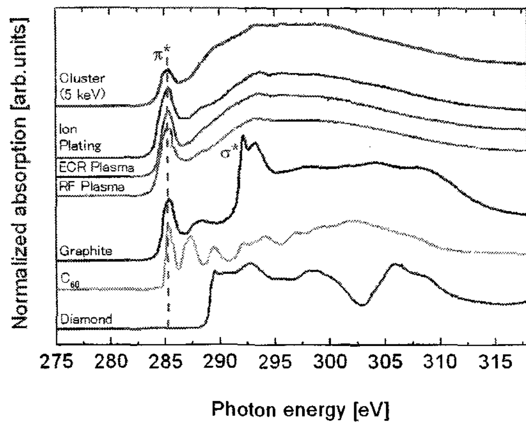

Figure 3 NEXAFS spectra of various carbon materials. Transition of 1S to sp^2 bond was found on most of materials, except for diamond. The NEXAFS spectrum of DLC film deposited with Cluster Ion Assisted technique is quite different from that of C_{60} film. This indicates that C_{60} molecules were decomposed to form DLC film.

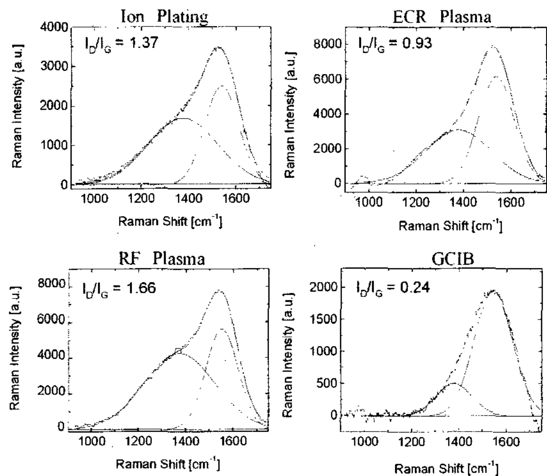

Figure 4 Raman spectra of DLC films deposited with various techniques. I(D) and I(G) peak were obtained from the peak deconvolution of Raman spectra. The I(D)/I(G) ratio is also shown. I(D)/I(G) ratio depend on the deposition technique.

simultaneously irradiated with energetic Ar cluster ions was completely different from that of the C_{60} film. Deposited C_{60} molecules were decomposed by the collisions of Ar cluster ions on the surface, and a DLC film containing large amounts of sp^3 bond was formed.

Figure 4 shows Raman spectra of films deposited with various ion assisted deposition technique. Raman spectra of the DLC films were generally evaluated with D (1350cm^{-1}) and G (1550cm^{-1}) peaks for an estimation of sp^2 contents. The D peak is usually assigned to A_{1g} zone-edge mode, because of the finite size of the graphitic domains. G peak is originated from the zone-center E_{2g} photon, which means the lattice vibrations in the plane of the graphite-like rings [29-31]. I(D)/I(G) peak ratios were obtained from the peak deconvolution of Raman spectra. When the I(D)/I(G) ratio is small, it is generally believed that there is only a small amount of sp^2 content in the DLC film[32]. The I(D)/I(G) ratio depends on the deposition technique. The I(D)/I(G) ratio obtained with Raman is compared with EELS, NEXAFS resultsin Table I. EELS, NEXAFS and Raman results are in good agreement. A film with a small amount of sp^2 bond is much harder than tha with

Table I sp^2 content measured with EELS and NEXAFS and I(D)/I(G) ratio. EELS, NEXAFS and Raman results are in good agreement. The film, with a small amount of sp^2 bond is much harder than that with a large amount of sp^2 bond.

	sp^2 Content (NEXAFS)	sp^2 Content (EELS)	I_D/I_GRatio (Raman)
RF Plasma	1	–	1.66
Ion Plating	0.88	1	1.37
ECR Plasma	0.88	0.98	0.93
Cluster (5 keV)	0.59	0.76	0.16

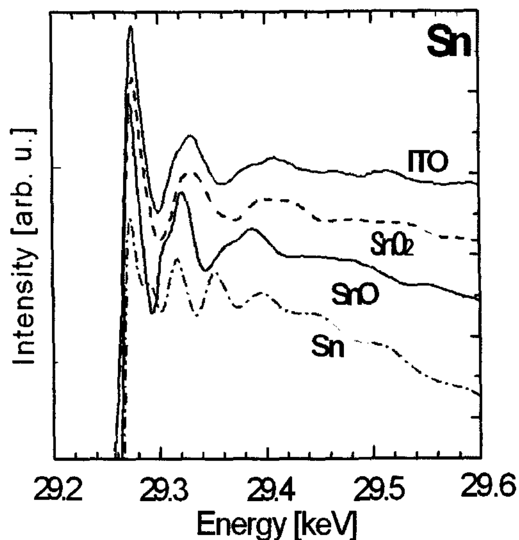

Figure 5 EXAFS spectra of various materials. The spectrum of ITO is completely different from that of tin oxide.

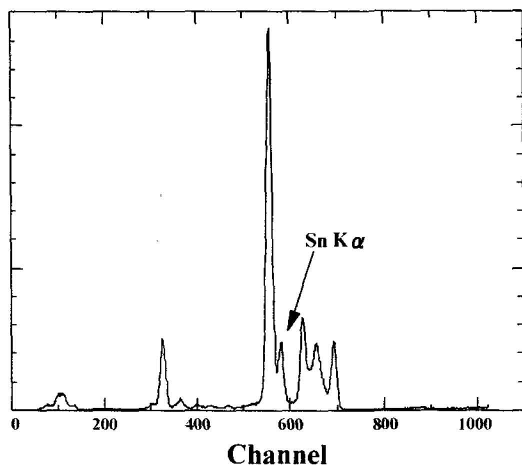

Figure 6 Typical X-ray fluorescence spectrum of ITO film. The largest peak corresponds to In Kα fluorescence. The Sn Kα fluorescence signal is near In Kα fluorescence. Single channel analyzer (SCA) is used to select Sn Kα fluorescence from the spectra.

large amount of sp^2 bond. DLC film formed with the cluster ion assisted technique is the hardest and exhibits the lowest sp^2 bond content in all samples.

3.2 ITO films

Sn K EXAFS spectra of various materials are shown in figure 5. All spectra shown in this figure were measured with the transmission technique. More than 5 ITO samples were stacked in order to obtain enough absorbance of X-ray near the Sn K edge. The quality of the ITO samples is quite poor, because of the very high deposition rate. According to the electrical measurement, most of Sn atoms are electrically inactivated in the films used in this measurement. Nevertheless, the ITO spectrum is quite different from Sn metal foil and tin oxides. This result indicates that no segregation of Sn atoms occurs in ITO films. Even though Sn atoms are electrically inactivated, the local structure around Sn atoms in ITO is completely different from the in oxide structure. Electrically inactive Sn atoms seem to be located on the lattice site of In_2O_3. However, it is very difficult to measure highly conductive ITO films in which Sn atoms are electrically activated, because the thickness of these films is usually less than 1μm. Therefore, the X-ray fluorescence technique was used to measure EXAFS spectra.

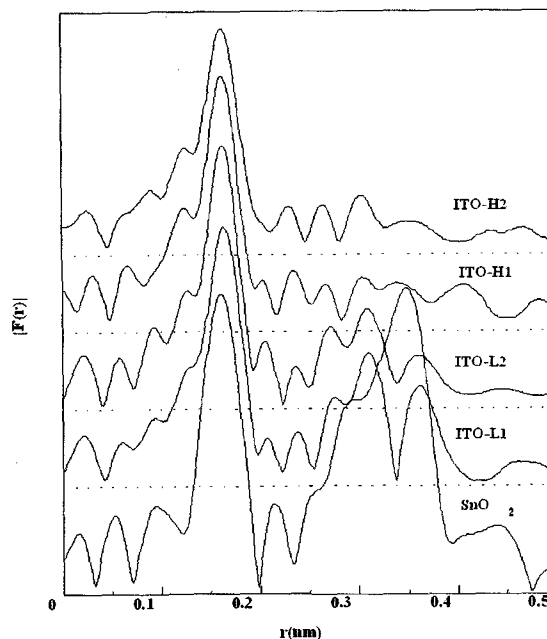

Figure 7 The radial structure function |F(r)| of ITO films and SnO_2 calculated with Fourier transform analysis of Sn K EXAFS spectra.

Typical X-ray fluorescence spectrum of ITO films is shown in figure 6. Multi channel analyzer (MCA) was used to measure this spectrum. Sn Kα fluorescence signal near In Kα fluorescence is depicted in figure 5. In order to measure the EXAFS spectra, Sn Kα fluorescence signal has to be selected. However, thin foil filtering technique could not be useful, because Sn Kα fluorescence has a higher energy than the In Kα fluorescence. Single channel analyzer (SCA) is used to select Sn Kα fluorescence from SSD.

Fourier transform analysis has been applied to Sn K EXAFS spectra. The range of Fourier transformation region was from 37.2 to 135.4 nm^{-1} in k space. The radial structure function |F(r)| of ITO films and SnO_2 is shown in Fig. 7. Since the phase shift parameter and the correction for the inner potential energy were not included in these calculations, the peaks in the |F(r)| curves are found at slightly shorter distances than those in the actual structures.

The first peaks around 0.16 nm in Fig. 7 correspond to Sn-O bonds, and the shapes are different from those of SnO_2. This suggests that the coordination state of tin in ITO films is different from tin in SnO_2. The second peaks correspond to Sn-In and the second nearest Sn-O. The second peaks are more characteristic than the first peaks.

The second peak becomes large, when the substrate

Table II The first interatomic distances, coordination numbers, growth temperature and resistivity of the films. Crystal structure of SnO_2 is rutile-type. Sn in SnO_2 has six nearest oxygen atoms located at 0.2052nm. The average coordination number increases with substrate temperature. This tendency indicates that ITO film is well oxidized at high temperature.

Samples	N	r(nm)	σ(nm)	Temp. (°C)	Resistivity (Ω·cm)	O2 gas cluster ion
SnO2	6	0.2052	0.0055(14)			
ITO-H1	5.0(1)	0.2071(1)	0.0057(11)	300	1.3×10^{-4}	irradiated
ITO-H2	4.9(1)	0.2064(1)	0.0055(12)	200	1.7×10^{-4}	irradiated
ITO-L1	4.6(1)	0.2052(1)	0.0056(12)	R.T.	1.2×10^{-3}	irradiated
ITO-L2	4.1(1)	0.2059(1)	0.0058(12)	R.T.	3.0×10^{-3}	unirradiated

temperature during deposition is more than 200C. The spectra of ITO-L1 and ITO-L2 films deposited at room temperature have no peak at the same distance. This is consistent with the result of X-ray diffraction. Amorphous ITO films are formed when the substrate temperature is less than 200C.

The first peaks of |F(r)| curves were inversely transformed to obtain $k^3\chi_1(k)$. The $k^3\chi_1(k)$ were fitted with the theoretical values for the phase shift and the amplitude parameters. We assumed that Sn atoms are located at substitution site of In_2O_3. The crystalline structure of In_2O_3 is bixbyite and has two different indium sites[33]. One is called b-site, and the other is d-site. The In atom is surounded by six oxygen atoms with an average distance of 0.218nm at both sides. In K EXAFS analysis of ITO films shows good agreement with that of In_2O_3 powder. The first interatomic distances, the coordination numbers, and the temperature factors of samples were obtained by fitting the calculated and observed $k^3\chi_1(k)$. In this calculation Teo and Lee's parameters [34] were employed. Table II shows the first interatomic distances, the coordination numbers, growth temperature and resistivity of the films. In order to compare with ITO and SnO_2, the first peaks of |F(r)| curves were analyzed in the same way with adopting crystalline SnO_2 as a reference. Crystal structure of SnO_2 is rutile-type. Sn in SnO_2 has six nearest oxygen atoms located at 0.2052nm.

The average coordination number increases with substrate temperature. This tendency indicates that the ITO film is well oxidized at high temperature. The average coordination number of ITO-L1 is very much lower than that of ITO-L2. The difference in growth condition of these films is cluster ion irradiation. Transparent ITO film can be grown with cluster ion irradiation even at room temperature. However, dark ITO film is grown without cluster ion irradiation, and the stoichiometry of the films is not kept. This result agrees well to the coordination number calculated from EXAFS. Oxygen cluster ion beam has a great capability to oxidize surfaces.

The Sn-O distance slightly increases for the films grown at high substrate temperature. The structure of ITO film is considered to be also bixbyite-type structure in which a part of In is substituted by Sn [35]. The ionic radius of In is larger than that of Sn. The substitution of In by Sn may increase Sn-O distance. Therefore EXAFS result for the Sn-O distance shows progress of the substitution. The substitution of trivalent ion by tetravalent ion creates carrier in ITO film. The decrease of resistivity with increasing of substrate temperature during deposition may be due to this reason.

4. SUMMARY

Gas Cluster Ion Beam (GCIB) assisted deposition was developed to deposit DLC and ITO films, which have been investigated with XAFS technique. EELS, NEXAFS and Raman spectroscopy have been used to measure the sp^2 content in the films. Good correlation between EELS, NEXAFS and Raman spectroscopy was found. The local structure around Sn atoms in ITO films was investigated with Sn K EXAFS in both the transmission and the fluorescent technique. The local structure around Sn atoms in ITO is completely different from tin oxides structure. The first neighbor Sn-O distance was slightly increased with substrate temperature during deposition.

Acknowledgment

The authors thankfully acknowledge NEDO (New energy and industrial technology development organization) in Japan for supporting this work.

References

[1] I. Yamada, W.L. Brown, J.A. Northby and M. Sosnowski, *Nucl. Instr. and Meth. in Phys. Res. B*, **79**

223 (1993).
[2] I. Yamada, J. Matsuo, Z. Insepov, T. Aoki, T. Seki and N. Toyoda, *Nucl. Instr. and Meth. in Phys. Res. B*, **164/165**, 944-959 (2000).
[3] I. Yamada, J. Matsuo, N.Toyoda and A. Kirkpatrick, *Materials Science & Engineering*, **R34**, 231-295 (2001).
[4] W. Qin, R.P. Howson, M. Akizuki, J. Maastuo, G. Takaoka, and I. Yamada, *Material Chem.& Phys.*, **54**, 258 (1998).
[5] M. Akizuki, J. Matsuo, I. Yamada, M. Harada, S. Ogasawara and A. Doi, *Jpn. J. Appl. Phys.*, **35**, 1450 (1996).
[6] J. Matsuo, W. Qin, M. Akizuki, T. Yodoshi and I. Yamada, *Mat. Res. Soc. Symp. Proc.*, **504**, 87(1997)
[7] H. Kitani, N. Toyoda, J. Matsuo and I. Yamada, *Nucl. Instr. and Meth. in Phys. Res. B*, **121**, 489 (1997).
[8] J. Matsuo, H. Katsumata, E. Minami and I. Yamada, *Nucl. Instr. and Meth. in Phys. Res. B*, **161/163**, 952-957 (2000).
[9] J. Matsuo, D. Takeuchi, A. Kitani and I. Yamada, *Nucl. Instr. and Meth. in Phys. Res. B*, **112**, 89-93 (1996).
[10] K. Goto, J. Matsuo, Y. Tada, T. Sugii and I. Yamada, *IEEE Transactions on Electron Devices*, **46**, 683-689 (1999).
[11] A. Yoshida, M.Deguchi, M.Kitabatake, T.Hirao, J. Matsuo, N.Toyoda and I.Yamada, *Nucl. Instr. and Meth. in Phys. Res. B*, **112**, 248-251 (1996).
[12] A. Nishiyama, M.Adachi, N.Toyoda, N.Hagiwara, J. Matsuo and I.Yamada, *Applications of Accelerators in Research and Industry, The American Institute of Physics* **475**, 421-424 (1999).
[13] N.Toyoda, N.Hagiwara, J. Matsuo and I.Yamada, *Nucl. Instr. and Meth. in Phys. Res. B*, **148**, 639-644 (1999).
[14] J. Matsuo, M. Akizuki, J. Northby, G.H. Takaoka and I. Yamada, *Surface Review and Letters*, **3**, 1017-1021 (1996).
[15] T. Seki, M. Tanomura, T. Aoki, J. Matsuo, and I. Yamada, *Proc. of Materials Research Society Symposium*, **504**, 93 (1997).
[16] T.Aoki, T.Seki, J. Matsuo, Z.Insepov and I.Yamada, *Nucl. Instr. and Meth. in Phys. Res. B*, **153**, 264-269 (1999).
[17] T. Aoki, J. Matsuo, Z. Insepov and I. Yamada, *Nucl. Instr. and Meth. in Phys. Res. B*, **121**, 49 (1997).
[18] J. J. Sun, K. Shimazawa, N. Kasahara, K. Sato, T. Kagami, S. Saruki, S. Araki, and M. Matsuzaki, *J. App.Phys*, **89**, 6653 (2001).
[19] T. Kitagawa, I. Yamada, N. Toyoda, H. Tsubakino, J. Matsuo, G.H. Takaoka, and Allen Kirkpatrick, *Nucl. Instr. and Meth. in Phys. Res. B*, submitted.
[20] K. Kanda, T. Kitagawa, Y. Shimizugawa, Y. Haruyama, S. Matsui, M. Terasawa, H. Tsubakino, I. Yamada, T. Gejo, and M. Kamada, *Jpn. J. Appl. Phys.*, **41**, 4295 (2002).
[21] J. Ullmann, *Nucl. Instr. and Meth. in Phys. Res. B*, **127**, 910 (1997).
[22] H. Tsai and D.B. Bogy, *J. Vac. Sci. Technol. A*, **5**, 3287 (1987).
[23] T.W. Scharf, R.D. Ott, D. Yang, and J.A. Barnard, *J. Appl. Phys.*, **85**, 3142, (1999).
[24] F. Hagena, *Rev. Sci. Instrum.*, **63**, 2374 (1992).
[25] R. Beuhler and L. Friedman, *Chem.Rev.*, **86**, 521 (1986).
[26] C.Lenardi, P. Piseri, V. Briois, C.E. Bottani, A. Li Bassi, P. Milani, *J. Appl. Phys.*, **85**, 7159 (1999).
[27] P. Lespade, A. Marchard, M. Couzi, and F. Cruege, *Carbon*, **22**, 375 (1984).
[28] L.J.Terminello, D.K. Shuh, F.J.Himpsel, D.A. Lapiano-Smith, J.Stohr, D.S. Bethune and G. Meijer, *Chem. Phys. Lett.*, **82**, 491 (1991).
[29] F. Tuinstra and J. L. Koenig, *J. Chem. Phys.*, **53**, 1126 (1970).
[30] R. J. Nemanich and S. A. Solin, *Phys. Rev. B*, **20**, 392 (1979).
[31] P. Lespade, R. Al-Jishi, and M. S. Dresselhaus, *Carbon*, **20**, 427 (1982).
[32] D. G. McCulloch, D. R. McKenzie, S. Prawer, A. R. Merchant, E. G. Gerstner, and R. Kalish, *Diam. Relat. Mater.*, **6**, 1622 (1997).
[33] M. Marezio, *Acta Cryst.*, **20** 723 (1966).
[34] B. K. Teo and P. A. Lee, *J. Am. Chem. Soc.*, **101**, 2815 (1979).
[35] I. Hamberg and C.G. Granqvist, *J. Appl. Phys.*, **60**, R123 (1986).

(Received August 8, 2003; Accepted August 21, 2003)